Indian Journal of Electrical Engineering and Informatics (IJEEI)
Vol.2.No.1 2014pp 25-32
available at: www.goniv.com
Paper Received :05-03-2014
Paper Published:28-03-2014
Paper Reviewed by: 1. John Arhter 2. Hendry Goyal
Editor : Prof. P.Muthukumar

A HIGH STEP-UP FULL BRIDGE THREE PORT DC-DC CONVERTER WITH WIDE INPUT VOLTAGE RANGE FOR RENEWABLE ENERGY SYSTEM

[1]N.MAHESWARI, [2]B.MEENAKSHI SUNDARAM
Department of Power Electronics and Drives
Sethu Institute of Technology,
Pulloor, Kariapatti-626115.

ABSTRACT

In this paper concentrates on the implementation and operation of a Full-Bridge Three Port Dc-Dc converter. Using this proposed method is developed for renewable power system applications which feature simple topology and control, a reduced number of devices and single-stage power conversion between any two of three ports. The proposed method split into two switching legs of the FBC into two switching cells with different sources and allows a dc bias current in the transformer. The proposed method consists of two bidirectional ports and one isolated port. The primary circuit of the proposed method functions as a buck-boost converter and provides power flow path between the ports on the primary side. The proposed method can adapt to wide source voltage range and tight control over two of three ports can achieve and the third port provides the power balance and using Maximum Power Point Tracking (MPPT) with results from Fuzzy control techniques.

Index Terms— MPPT - Fuzzy logic - Photovoltaic system, Boost-Buck DC-DC Converter, full bridge Three Port Converter, Renewable energy system.

1. INTRODUCTION

Renewable power systems, which are capable of harvesting energy from, for example, solar cells, fuel cells, wind, and thermoelectric generators, are found in many applications such as hybrid electric vehicles, satellites, traffic lights, and powering remote communication systems. Since the output power of renewable sources is stochastic and the sources lack energy storage capabilities, energy storage systems such as a battery or a super capacitor are required to improve the system dynamics and steady-state characteristics. A three-port converter (TPC) which can interface with renewable sources, storage elements and loads. Compared with the conventional Multiple-input converters have been proposed as a cost-effective and flexible way to interface various sources and, in some cases, energy-storage devices, with a load. The topologies described in these works can be divided into two categories according to whether the connection between inputs is performed through a magnetic coupling in a transformer or not. Integrated multiport converters for interfacing several power sources and storage devices are widely used in recent years. Instead of using individual power electronic converters for each of the energy sources, multiport converters have the advantages including less components, lower cost, more compact size, and better dynamic performance. In many cases, at least one energy storage device should be incorporated. For example, in the electric vehicle application, the regenerative energy occurs during acceleration or startup. Therefore, it is very important for the port connected to the energy storage to allow bidirectional power flow. Various kinds of topologies have been proposed due to the advantages of multiport converters. The combination strategies for the multiport converter include sharing switches, capacitors, inductors, or magnetic cores [1]. One could select a proper topology by considering many aspects such as cost, reliability, and flexibility depending on the applications. Many multiport converter topologies have been presented in the literature and can be roughly divided into two categories. One is non isolated type [2]–[10]: the non isolated converters are usually derived from the typical buck, boost, or buck–boost topologies and are more compact in size. The other is isolated type [11]–

[20]: the isolated converters using bridge topologies and multiwinding transformers to match wide input voltage ranges. Many isolated three-port converters with half-bridge [12]–[14] or full bridge [15]–[18] topologies are suitable for high step-up applications since a multiwinding transformer is adopted. These isolated three-port converters could achieve galvanic isolation and bidirectional capabilities but the amount of active switches results in complicated driving circuits and large size. A converter based on the boost-dual-half bridge topology is presented in [12]. Integrated three-port converters derived from a half-bridge converter are presented in [19]–[21] to interface PV and battery power. Small-signal modeling and decoupling network is introduced in [20] to design the compensators separately for the cross-coupled control loops. A family of three-port half-bridge converters is described in [21] and the primary circuit can function as a synchronous rectification buck converter. Therefore, the converters in [19]–[21] are suitable for stand-alone step-down applications. The major contribution of this paper is to propose a systematic method for generating TPC topologies from FBCs and to find a novel full-bridge TPC (FB-TPC) with single-stage power conversion between any two of the three ports. Furthermore, from a topological point of view, because a buck-boost converter is integrated in the proposed FB-TPC, it can adapt to applications with a wide source voltage range. ZVS of all the Primary-side switches can also be achieved with the proposed FB-TPC.

2. DISCRIPTION AND OPERATING PRINCILPE OF THE FB-TPC FOR THE STAND-ALONE RENEWABLE POWER SYSTEM APPLICATION

The primary side of the FBC consists of two switching legs, composed of SA1, SA2 and SB 1, SB 2, in parallel, connected to a common input source Vsa and Vsb. Close observation indicates that the FB-TPC has a symmetrical structure and both Vsa and Vsb can supply power to the load Vo. In addition, a bidirectional buck-boost converter is also integrated in the primary side of the FB-TPC by employing the magnetizing inductor of the transformer Lm as a filter inductor. With the bidirectional buck-boost converter, the power flow paths between the two sources, Vsa and Vsb, can be configured and the power can be transferred between Vsa and Vsb freely.

The FB-TPC, as shown in Fig. 1, is applied to a stand-alone PV power system with battery backup to verify the proposed topology. To better analyze the operation principle, the proposed FB-TPC topology is redrawn, the two source ports are connected to a PV source and a battery, respectively, while the output port is connected to a load. There are three power flows in the standalone PV power system: 1) from PV to load; 2) from PV to battery; and 3) from battery to load.

As for the FB-TPC, the load port usually has to be tightly regulated to meet the load requirements, while the input port from the PV source should implement the maximum power tracking to harvest the most energy. Therefore, the mismatch in power between the PV source and load has to be charged into or discharged from the battery port, which means that in the FBTPC, two of the three ports should be controlled independently and the third one used for power balance.

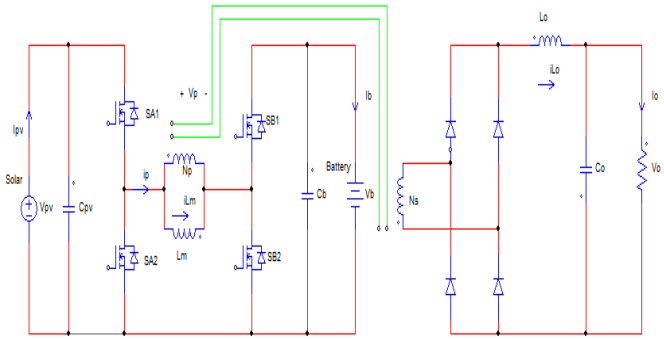

Fig: 1 Topology of the proposed FB-TPC.

As a result, two independently controlled variables are necessary.

A. Switching State Analysis

Ignoring the power loss in the conversion, we have

$$Ppv = Pb + Po \qquad (1)$$

Where Ppv, Pb , and Po are the power flows through the PV, battery, and load port, respectively. The FB-TPC has three possible operation modes: 1) dual-output (DO) mode, with Ppv ≥ Po, the battery absorbs the surplus solar power and both the load and battery take the power from PV; (2) dual-input (DI) mode, with Ppv ≤ Po and Ppv > 0, the battery discharges to feed the load along with the PV (3) single-input single-output (SISO) mode, with Ppv = 0, the battery supplies the load power alone. When Ppv = Po exactly, the solar supplies the load power alone and the converter operates in a boundary state of DI and DO modes. This state can either be treated as DI or DO mode. Since the FB-TPC has a symmetrical structure, the operation of the converter in this state is the same as that of SISO mode, where the battery feeds the load alone. The switching states in different operation modes are the same and the difference between these modes are the value and direction of iLm, as shown in Fig. 3, which is dependent on the power of ppv and po . In the DO mode, iLm is positive, in the SISO mode, iLm is negative, and in the DI mode, iLm can either be positive or negative.

For simplicity, the following assumptions are made: 1) Cpv ,Cb , and Co are large enough and the voltages of the three ports,Vpv , Vb , and Vo , are constant during the steady state; and 2) the Vpv ≥ Vb case is taken as an example for the switching state analysis. There are four switching states in one switching cycle. The key waveforms and the equivalent circuit in each state are shown in Figs. 2.

State I $t_0 - t_1$*]:* Before t_0, SA2 and SB 2 are ON and SA1 and SB 1 are OFF, while iLm freewheels through SA2 and SB 2. At t_0 , SA1 turns ON and SA2 turns OFF. A positive voltage is applied across the transformer's primary winding [see Fig. 3(a)]

$$\frac{di_{lm}}{dt} = \frac{V_{pv}}{L_m}$$

$$\frac{di_{Lo}}{dt} = \frac{nV_{pv} - Vo}{Lo} \qquad (2)$$

$$i_p = i_{Lm} + ni_{Lo}$$

State II $[t_1 - t_2]$*:* At t_1, SB2 turns OFF and SB1 turns ON. A positive voltage is applied on the primary winding of the transformer [see Fig. 3(b)]

$$\frac{di_{lm}}{dt} = \frac{V_{pv} - V_b}{L_m}$$

$$\frac{di_{Lo}}{dt} = \frac{n\left(V_{pv} - Vo \right) - V_b}{Lo} \qquad (3)$$

$$i_p = i_{Lm} + ni_{Lo}$$

State III $[t2 - t3]$*:* At *t*2, *SA*1 turns OFF and *SA*2 turns ON. A negative voltage is applied on the primary winding of the transformer Fig. 3(c)

$$\frac{di_{lm}}{dt} = -\frac{V_b}{L_m}$$

$$\frac{di_{Lo}}{dt} = \frac{nV_b - Vo}{Lo} \qquad (4)$$

$$i_p = i_{Lm} - ni_{Lo}$$

State IV $[t_3 - t_4]$*:* At t3, SB1 turns OFF and SB2 turns ON. The Voltage across the primary winding is clamped at zero, and iLm freewheels through SA2 and SB2 [see Fig. 3(d)]

$$\frac{di_{lm}}{dt} = 0$$

$$\frac{di_{Lo}}{dt} = -\frac{Vo}{Lo} \qquad (5)$$

Applying the volt-second balance principle to the magnetizing Inductor of the transformer *Lm* and the output filter inductor *Lo*, respectively, we obtain that the following:

$$Vpv = \frac{DB1}{DA1} Vb$$

(6)

$$VO = n\,[D1Vpv + D2\,(Vpv - Vb) + D3Vb]$$
$$= 2nD3Vb \qquad (7)$$

TABLE I
Operation modes of FB-TPC

Operating Modes	**Power of PV**	**Power of Battery**
Dual-Output mode	Ppv > = Po	Battery Charging, Pb >= 0
Dual-input mode	Ppv < = Po , Ppv > 0	Battery Charging, Pb < 0
Single-input Single-Output mode	Ppv = 0	Battery discharging, Pb = -Po

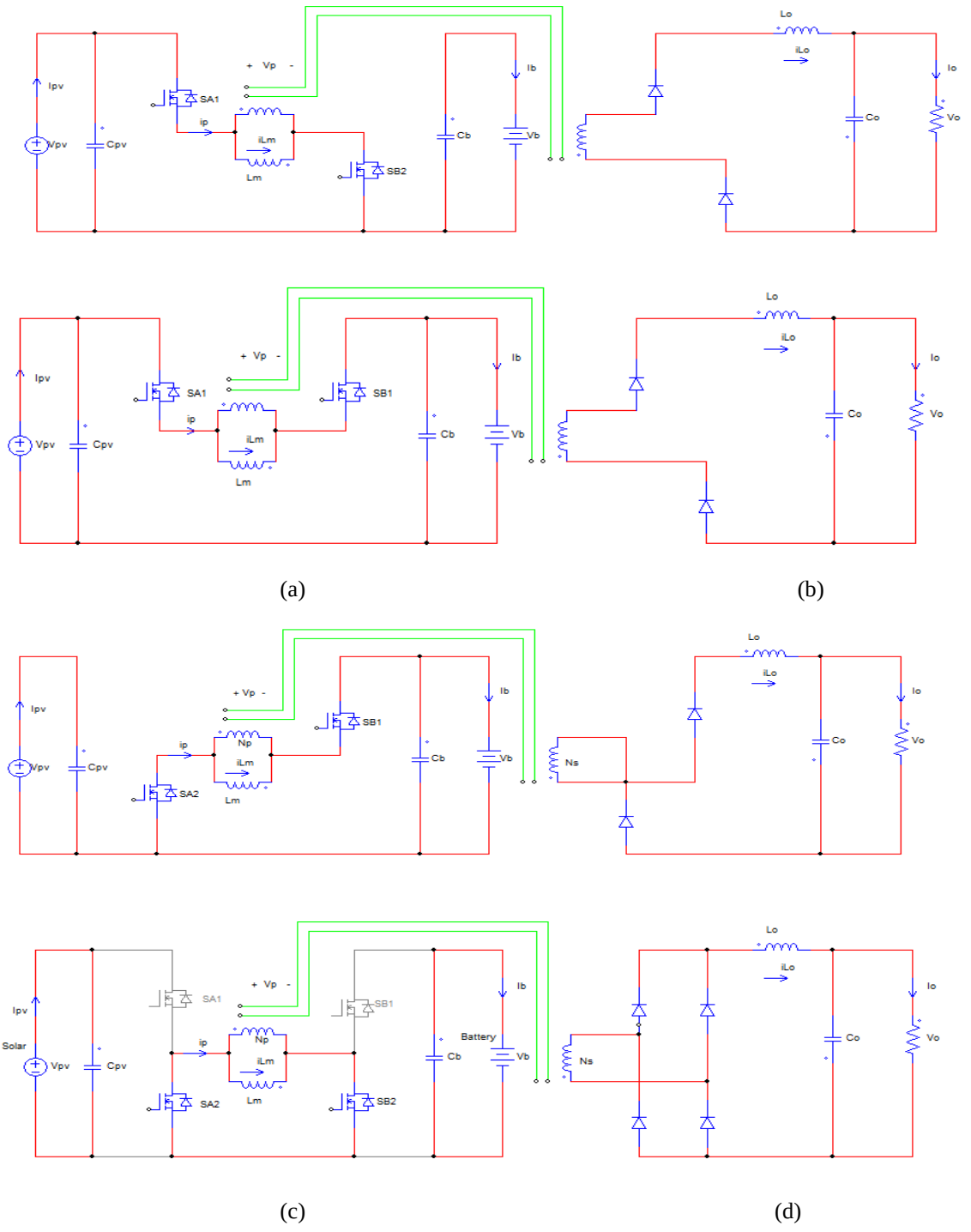

Fig.2. Equivalent circuits of each switching state. (a) [t_0, t_1]. (b) [t_1, t_2]. (c) [t_2, t_3]. (d) [t_3, t_4].

B. ZVS Analysis

According to the analysis, the operation of the FB-TPC is similar to the operation of a phase-shift FBC [23], [24] with the two switches SA1 (SB1) and SA2 (SB2), driven with complementary signals. The proposed FB-TPC can utilize the leakage inductance, filter inductance, and the output capacitors (parasitic drain to source capacitors) of the switches to realize ZVS, zero-voltage turn-ON, and zero-voltage turn-OFF for all the switches. The operation principle is similar to the phase-shift FBC [23], [24]. The only difference is that in the proposed FBTPC, the magnetizing inductor of the transformer Lm can also help to achieve ZVS of the switches if the direction of iLm is the same as i_p.

Take SA2 as an example. As shown in Fig. 7, where only the primary circuit is shown for simplicity, considering the leakage inductance Lk , when SB1 is ON and SA1 is turned OFF, iP = iLm + niLo, the energy stored in Lk and Lm will release to charge or discharge the parasitic drain to source capacitors of SA1 and SA2 .

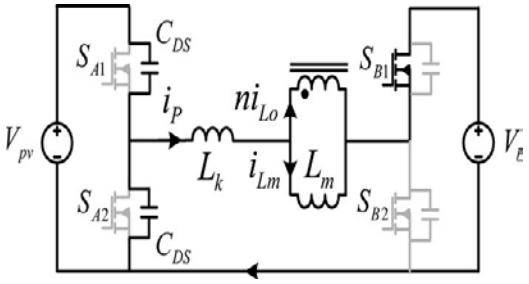

Fig 3 ZVS Analysis of SA2

As a result, with a proper dead time, ZVS of SA2 can be achieved if the following condition is satisfied

$$\frac{1}{2}\left[L_k\left(i_{Lm}+ni_{Lo}\right)^2+L_m i^2{}_{Lm}\right]>C_{DS}V_b{}^2$$

(8)

C. Design Consideration

As for the semiconductor device stress, the FB-TPC is similar to the traditional FBC. But a key difference between these two converters is that the magnetizing inductance of the transformer Lm is operated as an inductor as well. We also take the Vpv ≥ Vb case as an example for analysis.
From (1), in the steady state, we have

$$\text{Vpv Ipv} = \text{VbIb} + \text{Vo}$$

(9)
According to the switching states I and II, we have

$$\text{Ipv} = \text{DA1 (ILm + nIo)} \qquad (10)$$

Where ILm is the average magnetizing current of the transformer, and then we have

$$Ilm = \frac{Ipv}{DA1} - nIo \text{ Ipv}$$

(11)

From (11), it can be seen that the larger the DA1, the smaller the ILm.

According to the switching states II and III, we have

$$\text{Ib} = \text{D2 (ILm + nIo)} - \text{D3 (ILm} - \text{nIo)}$$
$$= \text{(DB1} - \text{2D3) ILm + DB1nIo.} \qquad (12)$$

Then the average transformer magnetizing current ILm can
also be given by the following equation:

$$Ilm = \frac{Ib - DB1nIo}{DB1 - 2D3}$$

(13)

According to (6), D3 is determined by Vb and VO, therefore, the larger the DB 1 the smaller the ILm.

It is noticed that ILm can be reduced by increasing the nominal values of DA1 and DB 1; this result is also valid for the Vpv <Vb case by following the same analysis procedure. Therefore, the value of ILm can be decreased with a properly designed modulation scheme.

4. SIMU LATION RESULTS

The Proposed method simulation results are shown in below.PV technology classified in to silicon crystalline technology and thin film technology. In this proposed method silicon crystalline is used. In this model 24v is obtained by connecting 40 cells each having 0.6v connected in series.

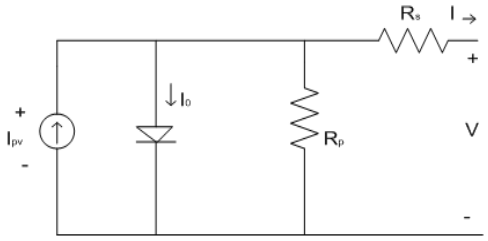

Fig. 4 PV Equivalent Circuit

The PV array is constructed by many series or parallel connections of solar cells. Each solar cell is formed by a PN junction semiconductor, which can produce currents by photovoltaic effects. The equivalent circuit of PV is shown in the figure (5).The current and voltage characteristics of solar cell are given by equations (i) and (ii).

$$I = I_{ph} - I_D$$

(i)

$$I = I_{sc} - I_o\left\{\exp\left[\left(q\left(V+R_sI\right)\right)/nK\right]-1\right\}\left(\left(V+R_sI\right)/R_{sh}\right)$$

(ii)

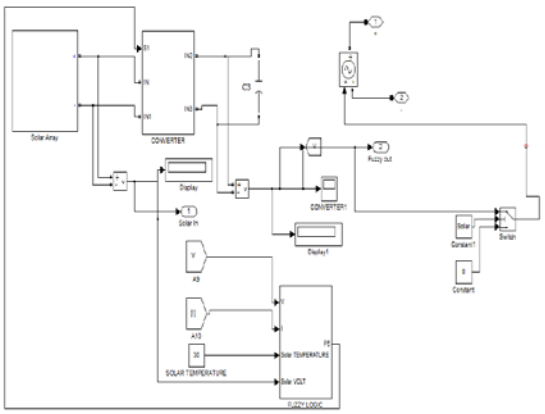

Fig. 5 Simulink model of a PV cell with boost converter and Fuzzy Logic

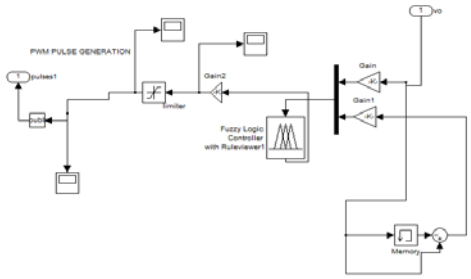

Fig.6 Block diagram of Fuzzy logic for MPPT

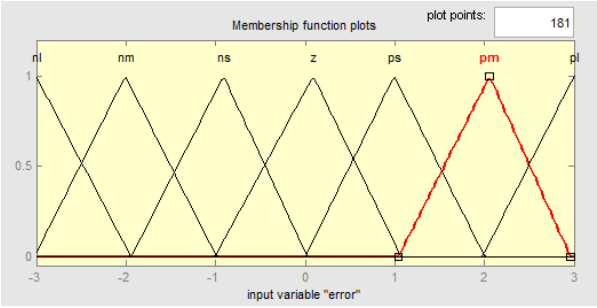

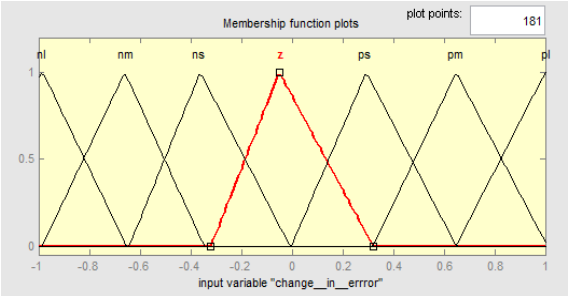

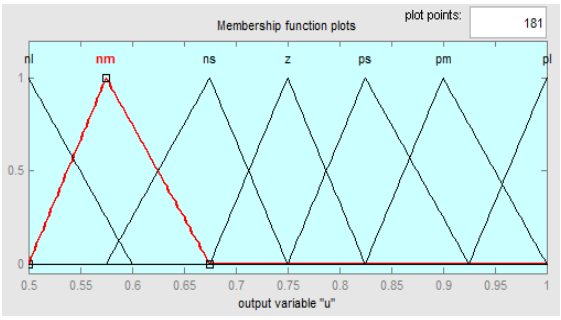

Fig. 7 Membership functions for (a) Input variable Error (b) Change in Error (c) Output variable

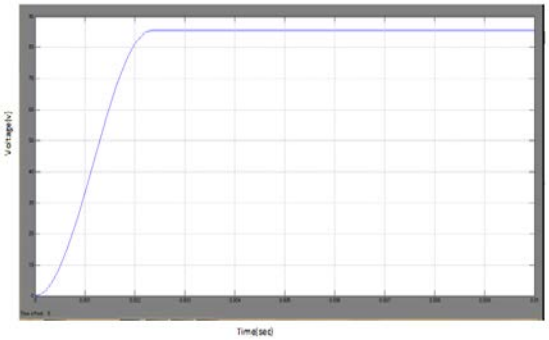

Fig 8 Input Voltage

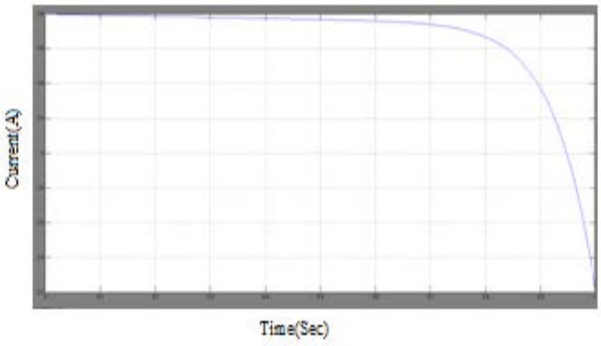

Fig 9 Input Current

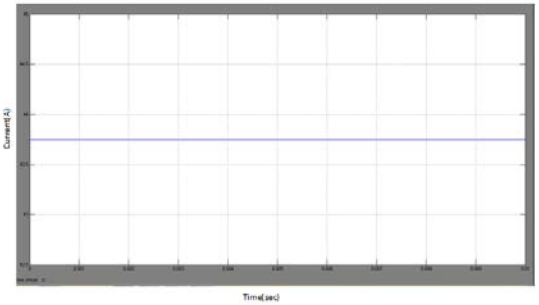

Fig 10 Output Current

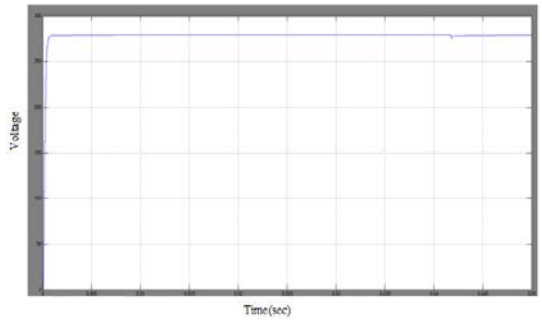

Fig 11 Output Voltage

4. CONCLUSION

In this proposed method, Photovoltaic system and Battery storage elements are used. In PV power generation is supplied to load excess power will stored in battery, if PV power is not sufficient that time battery fully supplied to load. In addition, the designed converter fuzzy control system is highly stable for the all possible operation of MPPT. The simulation results show, the converter control system provides good transient and steady state responses for the converter with respect to the different step changes in the PV power generation and the load condition. The proposed converter has the merits of making use of low voltage batteries, working in constant margin operating points in addition to the advantages of bidirectional power flow at the storage port, simple construction and low-power components.

REFERENCES

[1] S. H. Choung and A. Kwasinski, "Multiple-input DC-DC converter topologies comparison," in *Proc. 34th Annu. Conf. IEEE Ind. Electron.*,2008, pp. 2359–2364.

[2] W. G. Imes and F. D. Rodriguez, "A two-input tri-state converter for spacecraft power conditioning," in *Proc. AIAA Int. Energy Convers. Eng. Conf.*,1994, pp. 163–168.

[3] F. D. Rodriguez and W. G. Imes, "Analysis and modeling of a two input DC/DC converter with two controlled variables and four switched networks," in *Proc. AIAA Int. Energy Conf.*, 1994, pp. 163–168.

[4] B. G. Dobbs and P. L. Chapman, "A multiple-input DC–DC converter topology," *IEEE Power Electron. Lett.*, vol. 1, no. 1, pp. 6–9, Mar. 2003.

[5] R. J. Wai, Ch. Y. Lin, J. J. Liaw, and Y. R. Chang, "Newly designed ZVS multi-input converter," *IEEE Trans. Ind. Electron.*, vol. 58, no. 2, pp. 555–566, Feb. 2011

[6] L. Solero, A. Lidozzi, and J. A. Pomilio, "Design of multiple-input power converter for hybrid vehicles," in *Proc. IEEE Appl. Power Electron. Conf.*, 2004, pp. 1145–1151

[7] F. Nejabatkhah, S. Danyali, S. H. Hosseini, M. Sabahi, and S. M. Niapour, "Modeling and control of a newthree-input DC-DC boost converter for hybrid PV/FC/battery power system," *IEEE Trans. Power Electron.*, vol. 23, no. 2, pp. 782–792, Mar. 2008.

[8] J. Jung and A. Kwasinski, "A multiple-input SEPIC with a bi-directional input for modular distributed generation and energy storage integration," in *Proc. IEEE Appl. Power Electron. Conf.*, 2011, pp. 28–34.

[9] G.-J. Su and F. Z. Peng, "A low cost, triple-voltage bus DC–DC converter for automotive applications," in *Proc. IEEE Appl. Power Electron. Conf.*,2005, pp. 1015–1021.

[10] A.Kwasinski, "Identification of feasible topologies for multiple-input DC-DC converters," *IEEE Trans. Power Electron.*, vol. 24, no. 3, pp. 856–861, Mar. 2009.

[11] S. Yu and A. Kwasinski, "Analysis of a soft-switching technique for isolated time-sharing multiple-input converters," in *Proc. IEEE Appl. Power Electron. Conf.*, 2012, pp. 844–851.

[12] D. Liu and H. Li, "A ZVS bi-directional DC–DC converter for multiple energy storage elements," *IEEE Trans. Power Electron.*, vol. 21, no. 5, pp. 1513–1517, Sep. 2006.

[13] H. Tao, A. Kotsopoulos, J. L. Duarte, and M. A. M. Hendrix, "Triplehalf-bridge bidirectional converter controlled by phase shift and PWM,"in *Proc. IEEE Appl. Power Electron. Conf.*, Mar. 2006, pp. 1256–1262.

[14] L. Wang, Z. Wang, and H. Li, "Asymmetrical duty cycle control and decoupled power flow design of a three-port bidirectional DC-DC converter for fuel cell vehicle application?," *IEEE Trans. Power Electron.*, vol. 27, no. 2, pp. 891–903, Feb. 2012.

[15] Y.-M. Chen,Y.-C. Liu, and F.-Y.Wu, "Multi-input DC/DC converter based on themultiwinding transformer for renewable energy applications," *IEEETrans. Ind. Appl.*, vol. 38, no. 4, pp. 1096–1104, Jul./Aug. 2002.

[16] H. Tao, A.Kotsopoulos, J. L.Duarte, andM. A. M.Hendrix, "Transformer coupled multiport ZVS bidirectional DC–DC converter with wide input range," *IEEE Trans. Power Electron.*, vol. 23, no. 2, pp. 771–781, Mar.2008.

[17] C. Zhao, S. D. Round, and J. W. Kolar, "An isolated three-port bidirectional DC–DC converter with decoupled power flow management," *IEEETrans. Power Electron.*, vol. 23, no. 5, pp. 2443–2453, Sep. 2008.

[18] H. Krishnaswami and N. Mohan, "Three-port series resonant DC-DC converter to interface renewable energy sources with bidirectional load and energy storage ports," *IEEE Trans.*

Power Electron., vol. 24, no. 10,pp. 2289–2297, Oct. 2009.

[19] H. Al-Atrash, F. Tian, and I. Batarseh, "Tri-modal half-bridge converter topology for three-port interface," *IEEE Trans. Power Electron.*, vol. 22, no. 1, pp. 341–345, Jan. 2007.

[20] Z. Qian, O. Abdel-Rahman, H. Al-Atrash, and I. Batarseh, "Modeling and control of three-port dc/dc converter interface for satellite applications," *IEEE Trans. Power Electron.*, vol. 25, no. 3, pp. 637–649, Mar.2010

[21] N. D. Benavides and P. L. Chapman, "Power budgeting of a multiple input buck–boost converter," *IEEE Trans. Power Electron.*, vol. 20, no. 6, pp. 1303–1309, Nov. 2005.